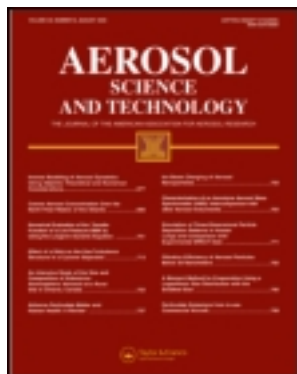


This article was downloaded by: [Institute of Earth Environment]

On: 23 September 2012, At: 23:41

Publisher: Taylor & Francis

Informa Ltd Registered in England and Wales Registered Number: 1072954 Registered office: Mortimer House, 37-41 Mortimer Street, London W1T 3JH, UK



Aerosol Science and Technology

Publication details, including instructions for authors and subscription information:

<http://www.tandfonline.com/loi/uast20>

The Influence of Dust on Quantitative Measurements of Black Carbon in Ice and Snow when Using a Thermal Optical Method

Mo Wang^a, Baiqing Xu^a, Huabiao Zhao^a, Junji Cao^b, Daniel Joswiak^a, Guangjian Wu^a & Shubiao Lin^a

^a Key Laboratory of Tibetan Environment Changes and Land Surface Processes, Institute of Tibetan Plateau Research, Chinese Academy of Sciences, Beijing, China

^b SKLLQG, Institute of Earth Environment, Chinese Academy of Sciences, Xi'an, China

Version of record first published: 28 Sep 2011.

To cite this article: Mo Wang, Baiqing Xu, Huabiao Zhao, Junji Cao, Daniel Joswiak, Guangjian Wu & Shubiao Lin (2012): The Influence of Dust on Quantitative Measurements of Black Carbon in Ice and Snow when Using a Thermal Optical Method, *Aerosol Science and Technology*, 46:1, 60-69

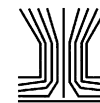
To link to this article: <http://dx.doi.org/10.1080/02786826.2011.605815>

PLEASE SCROLL DOWN FOR ARTICLE

Full terms and conditions of use: <http://www.tandfonline.com/page/terms-and-conditions>

This article may be used for research, teaching, and private study purposes. Any substantial or systematic reproduction, redistribution, reselling, loan, sub-licensing, systematic supply, or distribution in any form to anyone is expressly forbidden.

The publisher does not give any warranty express or implied or make any representation that the contents will be complete or accurate or up to date. The accuracy of any instructions, formulae, and drug doses should be independently verified with primary sources. The publisher shall not be liable for any loss, actions, claims, proceedings, demand, or costs or damages whatsoever or howsoever caused arising directly or indirectly in connection with or arising out of the use of this material.



The Influence of Dust on Quantitative Measurements of Black Carbon in Ice and Snow when Using a Thermal Optical Method

Mo Wang,¹ Baiqing Xu,¹ Huabiao Zhao,¹ Junji Cao,² Daniel Joswiak,¹ Guangjian Wu,¹ and Shubiao Lin¹

¹Key Laboratory of Tibetan Environment Changes and Land Surface Processes, Institute of Tibetan Plateau Research, Chinese Academy of Sciences, Beijing, China

²SKLLQG, Institute of Earth Environment, Chinese Academy of Sciences, Xi'an, China

Accurate measurements of black carbon concentrations in snow and ice are essential to quantify its impact on glacial melting and sequential climate forcing via snow albedo. However, snow and ice contain dust that may severely bias the precision of the elemental carbon (EC) and organic carbon (OC) measurements of filters with a thermal/optical method. To evaluate the effects of dust on black carbon analysis and to optimize filtration methods, meltwater from ice core and surface snow samples with variable dust content were filtered with different methods, including filtration of the entire material (including settling) and supernatant liquid, mechanical stirring and sonication, as well as utilization of single and double quartz filters. In this research, it is shown that dust can induce an extra decrease in optical reflectance during the 250°C heating stage in the thermal/optical method and an improper OC and EC split. To address this problem, a correction procedure was suggested and used to revise the OC and EC results. The OC, EC, and TC concentration variations from different filtration methods along the ice core depth and along surface snow elevation were illustrated. These results indicate that black carbon and dust generally mix as agglomerates. The agglomerate structure will contribute to the underestimation of EC and OC in the measurement. However, carbonaceous matter can be efficiently detached from dust particles by ultrasonic agitation of the meltwater samples, which significantly improves carbon volatilization during the thermal/optical analysis.

[Supplementary materials are available for this article. Go to the publisher's online edition of *Aerosol Science and Technology* to view the free supplementary files.]

INTRODUCTION

Carbonaceous aerosols have received much attention for their associated interactions with solar radiation, role as cloud condensation nuclei, effect on snow albedo, and consequences for climate modification (Hansen and Nazarenko 2004; Ramanathan and Carmichael 2008). Components of scavenged carbonaceous aerosols from the atmosphere are preserved in snow and ice by wet and dry deposition. Accurate measurements of carbonaceous particles in snow and glacier ice provide an effective way to obtain information related to organic carbon (OC) and elemental carbon (EC) (also called black carbon; BC) historical atmospheric concentrations and combustion sources, and are useful for validation of atmospheric circulation models (McConnell et al. 2007; Xu et al. 2009a, 2009b). In addition, these measurements are necessary for quantification of carbonaceous aerosol effects on snow albedo and accelerated snowmelt.

The results from measuring environmental carbonaceous particles, however, can be highly variable as they depend not only on source, combustion process, atmospheric age, and mixing state of samples (Countess 1990; Lioussé et al. 1993; Birch 1998), but also on the experimental procedures and analysis techniques (Countess 1990; Birch 1998; Puxbaum and Bauer 2001; Schmid et al. 2001). Comparisons and round robin tests of atmospheric carbon analysis have been previously undertaken to optimize measurements (Countess 1990; Lioussé et al. 1993; Birch 1998; Puxbaum and Bauer 2001; Schmid et al. 2001). In the “carbon conference” international aerosol carbon round robin test, the EC and OC values of urban aerosols performed comparably with most of the thermal and optical methods (Schmid et al. 2001). However, results of rural and alpine samples exhibited

Received 28 January 2011; accepted 29 May 2011.

This study was supported by the National Basic Research Program of China (2009CB723901) and the National Natural Science Foundation of China (40930526). We would like to thank the anonymous referees for their valuable comments, which were greatly helpful for improving the manuscript, and Dr. Susan Kaspari for her suggestions on the experiment.

Address correspondence to Mo Wang, Key Laboratory of Tibetan Environment Changes and Land Surface Processes, Institute of Tibetan Plateau Research, Chinese Academy of Sciences, 18 Shuangqing Road, Haidian District, Beijing 100085, China. E-mail: wangmo@itpcas.ac.cn

high variances between analysis methods and laboratories due to the different charring artifacts derived from the variation in thermal methods (Puxbaum and Bauer 2001).

Carbonaceous particles in the snow and ice from remote glaciers are typically collected on quartz-fiber filters. Water-insoluble organic carbon (WIOC) and elemental carbon are measured by two-step thermal procedures (Cachier and Pertuisot 1994; Xu et al. 2006) or by thermal/optical methods (Xu et al. 2009a, 2009b). Two-step temperature methods quantify the organic carbon on a filter sample that evolves at a lower temperature (340°C), whereas the elemental carbon is measured at a higher temperature (650°C). The thermal/optical methods quantify the volatilizing carbon at different temperatures and atmospheres and also monitor the charring of organic matter by observing the change in optical signals given that EC is the primary light-absorbing component in the aerosol phase (Lioussé et al. 1993). In comparison to solely thermal methods, the thermal/optical methods are more advanced for charring correction by light reflected from or transmitted through the filter during analysis.

As with other common light-absorbing particles in the atmosphere (Clarke and Noone 1985; Warren and Clarke 1990), dust trapped in snow or glacier ice will not only decrease the sensitivity of the instrument (Chow et al. 2001) but also bias the WIOC/EC split point during the analysis as demonstrated in this study. This bias is especially prevalent in samples containing obvious dust particles because the dust content may be several orders of magnitude higher than EC, while the absorption coefficient is 2 or 3 times of magnitude smaller (Warren and Clarke 1990; Hansen et al. 1993). If elemental carbon is quantified only by optical methods, such as using the Aethalometer (Hansen et al. 1984), dust resulting in extra attenuation will be mistaken for EC. In thermal/optical measurements, a negative error in EC coupled with a positive error in OC can be derived from a deviated light signal measuring charred organic carbon as the reflectance/transmittance of dust is irreversibly changing while temperature increases. If dust is excluded from the analysis entirely, the carbonaceous particles attached to dust will be lost, resulting in underestimated OC and EC values. Hansen et al. (1993) obtained black carbon concentrations by comparing optical transmission attenuation before and after combustion to separate the optical attenuation of black carbon from dust, and Lavanchy et al. (1999) incorporated this method in ice core samples to eliminate the influence of dust. In this study, black carbon was quantified in melt samples using different methods of filtration for a better understanding of: (1) the mixing state of carbonaceous particles with other particles in ice and snow, and (2) the effects of dust on WIOC (hereafter "OC" for short) and EC concentrations. The aim was also to optimize the filtration and processing methods for thermal/optical carbon analysis. From the discrepancies among results, an assessment of the previously outlined sources of measurement error was obtained.

MATERIALS AND METHODS

Samples and Preparation

During the winter of 2007, 2 ice cores (9 cm in diameter, 5.47 m and 55.03 m in length) were retrieved from the accumulation zone of the Noijin Kangsang glacier (29°2.1'N, 90°11.88'E, 5950 m a.s.l.) in the southern Tibetan Plateau (Figure 1a). The ice cores were packed in double-sealed polyethylene bags in the field and then transported frozen to the laboratory facilities at the Institute of the Tibetan Plateau Research (Lhasa campus) for analysis. The shorter core (comprised of 6 sections ranging in length from 63 cm to 115 cm) was selected for the ice sample measurements presented here.

In a walk-in freezer at -20°C, each section was cut into 3–5 subsections at ~20 cm intervals using a band saw. This resulted in twenty-seven subsections, labeled No. 1 to No. 27. Each subsection was then split lengthwise into 4 equal portions and marked A, B, C, and D (Figure 1b). Note that each of the 4 samples with the same serial number, for example No. 1, belong to the same subsection, i.e., ice fragments of the same depth. Therefore, there were 4 series of ice core samples. Unfortunately, 3 samples (No. 7, No. 10, and No. 11) were excluded from the analysis as they exhibited significant melting. Once the ice core partitioning was finished, all samples were transferred to a Class 1000 clean room at -15°C. The outermost layer (approximately 1 cm in thickness) of each sample was removed using a precleaned scalpel in a Class 100 laminar flow bench to eliminate possible contamination from drilling, transport, and storage. The inner parts of all samples were stored at a low temperature in a 1-L glass beaker precleaned with a mixing liquid (H₂O–K₂Cr₂O₇–H₂SO₄) and then with ultrapure water (Milli-Q, 18.2 MΩ) and preweighed. Samples were weighed, sealed with pieces of aluminum foil, and allowed to melt at room temperature in a Class 100 laminar flow bench.

The 6 snow samples used in this study weighed between 1,000 and 1,600 g and were sealed in double plastic bags along the elevation gradient (4,800, 4,900, 5,000, 5,100, 5,200, and 5,300 m a.s.l.) on Zuoqiupu glacier (97.00°E–97.03°E, 29.33°N–29.33°N) in the southeast Tibetan Plateau (Figure 1a) during the spring of 2010. The snow samples were kept frozen until arrival in the laboratory, where they were allowed to melt in a Class 100 laminar flow bench. Dust particles were found deposited at the bottom of the sample bags. Each sample was mixed intensively before being poured in equal amounts into 3 precleaned beakers; approximately 30 mL was also sealed in bottles and remained in melted state for future analysis by single-particle soot photometer (SP2). The water samples in beakers weighed an average of ~280 g.

The quartz fiber filters (Whatman® QMA) with pore sizes of 1 μm used in this experiment were 15 mm in diameter and heated for 8 h in a tubular oven at 800°C with an oxygen stream before filtration. Immediately after the ice and snow samples melted, the liquid samples were filtered in the clean bench.

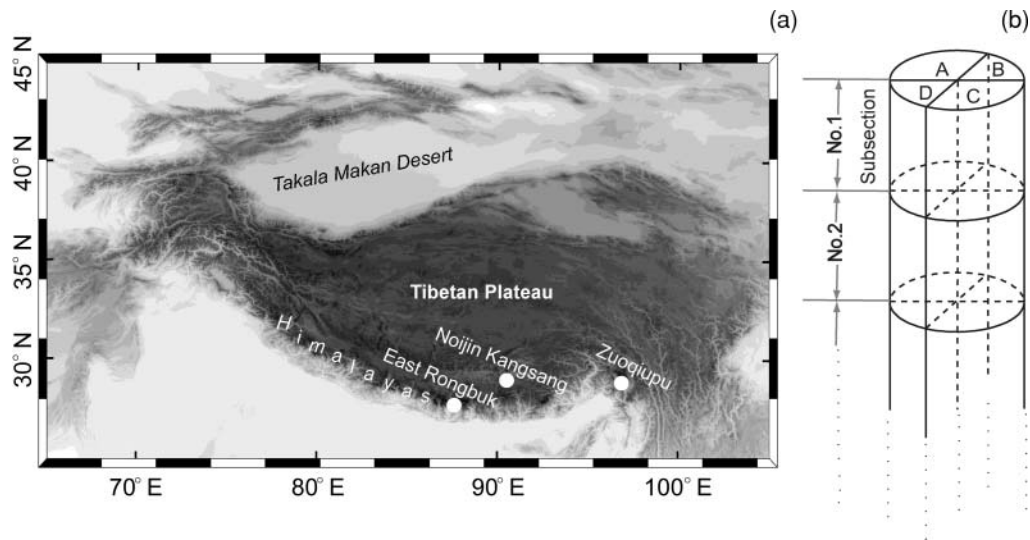


FIG. 1. (a) White dots indicate the sampling sites on East Rongbuk Glacier (Cong et al. 2008), the ice core drill site at Noijin Kangsang, and snow sample sites at Zuogijupu Glacier. (b) The ice core tubes were cut into twenty-four numbered subsections, split into 4 columns, and marked with capital letters.

Filtration was performed using a stainless-steel unit (400 mL volume) and resulted in a circular spot 10 mm in diameter (Xu et al. 2006).

Two sets of parallel experiments on ice and snow, both with different filtration methods, were conducted to understand the influence of dust on carbonaceous particle concentrations and to choose a proper filtering method for future ice core and snow research. The filtration methods, correspondingly named F_{ice-A} , F_{ice-B} , F_{ice-C} , and F_{ice-D} , for 4 ice sample series, and F_{snow-A} , F_{snow-B} , and F_{snow-C} , for 3 snow sample series, were carried out as follows (summarized in Table 1):

F_{ice-A} : Filter the samples directly including the water and dust particles.

F_{ice-B} : Stir the samples with a precleaned glass bar, allow them to settle for 10–15 min, and then filter the supernatant only.

F_{ice-C} : Same as F_{ice-B} , but filter the supernatant through superimposed double filters.

F_{ice-D} : Same as F_{ice-B} , but without stirring.

F_{snow-A} : Same as F_{ice-A} .

F_{snow-B} : Sonicate the samples for 15 min, allow them to settle, and filter the supernatant.

F_{snow-C} : Settle and filter the supernatant only.

The containers in F_{ice-A} and F_{snow-A} were rinsed 3 times with ultrapure water (Milli-Q 18.2 M Ω) to ensure complete transfer of particles to the filter. For the other filtration methods (F_{ice-B} , F_{ice-C} , F_{ice-D} , F_{snow-B} , and F_{snow-C}), the containers with the unfiltered dust particles were swirled 3 times using ~20 mL ultrapure water for each, allowed to settle for 10–15 min, and then the supernatant was pipetted for filtering. The 2 superimposed filters mentioned in the F_{ice-C} procedure were differentiated as C-I and C-II for the upper and lower filters, respectively.

Following filtration, the filter samples were removed into precleaned small glass containers with an inner diameter of ~1.5 cm. To remove inorganic carbonates that may interfere with EC determination, 50 μ L 0.1 M HCl was dropped onto the sample spot 3 times prior to analysis (Lavanchy et al. 1999).

TABLE 1
Summary of filtration processes

Filtration method	Sample category	Stirring method	Filtered material	Number of filters
F_{ice-A}	Ice	N/A	Supernatant liquid, sediment	1
F_{ice-B}	Ice	Glass bar	Supernatant liquid	1
F_{ice-C}	Ice	Glass bar	Supernatant liquid	2
F_{ice-D}	Ice	N/A	Supernatant liquid	1
F_{snow-A}	Snow	N/A	Supernatant liquid, sediment	1
F_{snow-B}	Snow	Ultrasonic	Supernatant liquid	1
F_{snow-C}	Snow	N/A	Supernatant liquid	1

The sample filters were then dried in the Class 100 laminar flow bench and stored for the next analysis.

The ice core subsections that did not contain visible dust particles in the meltwater comprised the Non-Dust Group ($n = 14$). There should be no difference between $F_{\text{ice-A}}$, $F_{\text{ice-B}}$, and $F_{\text{ice-D}}$; therefore, series A, B, and D can be considered repeats. For the other ice core subsections containing visible dust particles (Dust Group, $n = 10$), 2 issues will be addressed: 1) how the filtered dust particles influence the measured values of carbonaceous particle concentrations by comparing $F_{\text{ice-A}}$ to $F_{\text{ice-B}}$, and 2) whether the mechanical stirring of samples with a glass bar is an effective means to detach carbonaceous matter from the surface of dust particles by comparing $F_{\text{ice-B}}$ to $F_{\text{ice-D}}$ (assuming that OC and EC are attached to dust particles). By comparing $F_{\text{ice-C}}$ to the 3 other filtration methods, the collection efficiency of single filter membranes for carbonaceous particles was assessed.

As demonstrated in this study, mechanical stirring with a glass bar is not efficient for detaching black carbon from dust in ice core samples. Therefore, the snow melt samples in $F_{\text{snow-B}}$ were sonicated to separate carbonaceous particles and dust. By comparison among $F_{\text{snow-A}}$, $F_{\text{snow-B}}$, and $F_{\text{snow-C}}$, the amount of black carbon attached to dust particles and the associated mixing state can be recognized.

Carbonaceous Aerosol Analysis

All filter samples were analyzed for OC and EC by a Desert Research Institute (DRI) Model 2001 Thermal/Optical Carbon Analyzer following the IMPROVE TOR protocol (Chow et al. 1993; Chow and Watson 2002; Cao et al. 2008). This analysis system was tested in the international aerosol carbon round robin test stage I and provided OC and EC results comparable to most of the other analysis methods (Schmid et al. 2001). Each filter was punched in a 0.526 cm^2 area and then analyzed by the following 2 phases. In the first phase, the filter is combusted in a 100% nonoxidizing helium (He) atmosphere at 120°C , 250°C , 450°C , and 550°C to deliver 4 OC fractions that are OC1, OC2, OC3, and OC4, respectively. In the second phase, 2% O_2 is injected, and the temperature is raised from 550°C to 700°C and 800°C . This results in the production of 3 EC fractions (EC1, EC2, and EC3, respectively). As the temperature increases in the 100% He atmosphere, some of the OC pyrolyzes and darkens the filter deposit. This conversion process is monitored by measuring the reflectance and transmittance of light at 633 nm, which is produced with a He-Ne laser (Chow et al. 2004). When oxygen is added, the original and pyrolyzed black carbon combusts and the reflectance increases. The amount of carbon measured after oxygen addition until the reflectance attains the original value is reported as optically detected pyrolyzed organic carbon (POC). The IMPROVE protocol defines OC as $\text{OC1} + \text{OC2} + \text{OC3} + \text{OC4} + \text{POC}$ and EC as $\text{EC1} + \text{EC2} + \text{EC3} - \text{POC}$. TC (total carbon) is the sum of OC and EC. More simply stated, the carbon detected by the flame ionization detector (FID) before the

optical signal attains the initial value is defined as OC and after is defined as EC. Quality Assurance/Quality Control (QA/QC) procedures were followed as described in Cao et al. (2003).

Data Revision

According to the thermograms, the laser signal, which monitors the reflectivity of the filters, usually decreases as the temperature reaches 450°C but returns quickly at 550°C when 2% O_2 is introduced for most Non-Dust Group samples (Figure 2a). When dust particles are filtered with methods $F_{\text{ice-A}}$ and $F_{\text{snow-A}}$, the thermograms illustrate that the reflected light signal decreases in advance as the temperature reaches 250°C and does not return to the original value until the temperature reaches 700°C (Figure 2c), or even after the analysis for a few dusty samples (Figure 2d). Therefore, dust on the filter results in the FID division being postponed or inefficient. As a consequence, overestimated OC and underestimated or even negative EC values are produced.

In comparison with the thermogram of general carbonaceous aerosol samples in the atmosphere (Chow et al. 2004), there is an extra decrease in reflection at 250°C that can be attributed to dust on the filters. This result may be due to the minerals having optical properties that change at around 250°C . The dust-containing filters of ice core and snow samples present dark-brown and red-brown colors before and after combustion, respectively (online supplemental information, Figures S1 and S2), which likely indicates the existence of hematite (Lavanchy et al. 1999). The mineral dust in the atmosphere of the East Rongbuk Glacier is similar to the mineral particles recorded in the Noijin Gangsang ice core given the adjacent location under similar geologic conditions (Figure 1a). The elemental concentrations in the atmosphere measured on the East Rongbuk Glacier demonstrate that Fe is the second most abundant element after Ca (Cong et al. 2008), which points to the existence of hematite.

To test if hematite contributes to the decrease in optical signal at 250°C , approximately 45 mg Fe_2O_3 was weighed on a filter and combusted in the DRI Thermal/Optical Reflectance Carbon Analysis System; once to eliminate the possible carbonaceous matter in the hematite powder and then continually combusted a second time. In both first and second analysis thermograms, the light reflection signal revealed an obvious decrease at the 250°C temperature step with the same value maintained until the analysis completion (Figure 2b). This result indicates that the reflectance decrease at 250°C is probably derived from an optical property change of some minerals, such as hematite.

To eliminate the impact of dust on reflectance, the results were revised as follows. First, the initial reflectance value line was shifted parallel to the reflectance value directly after 250°C , i.e., right before the second obvious decrease in reflectance (black dotted lines in Figure 2c and d). After the reflectance achieved this obtained initial value, the carbon fraction volatilized from the filter sample was classified as EC.

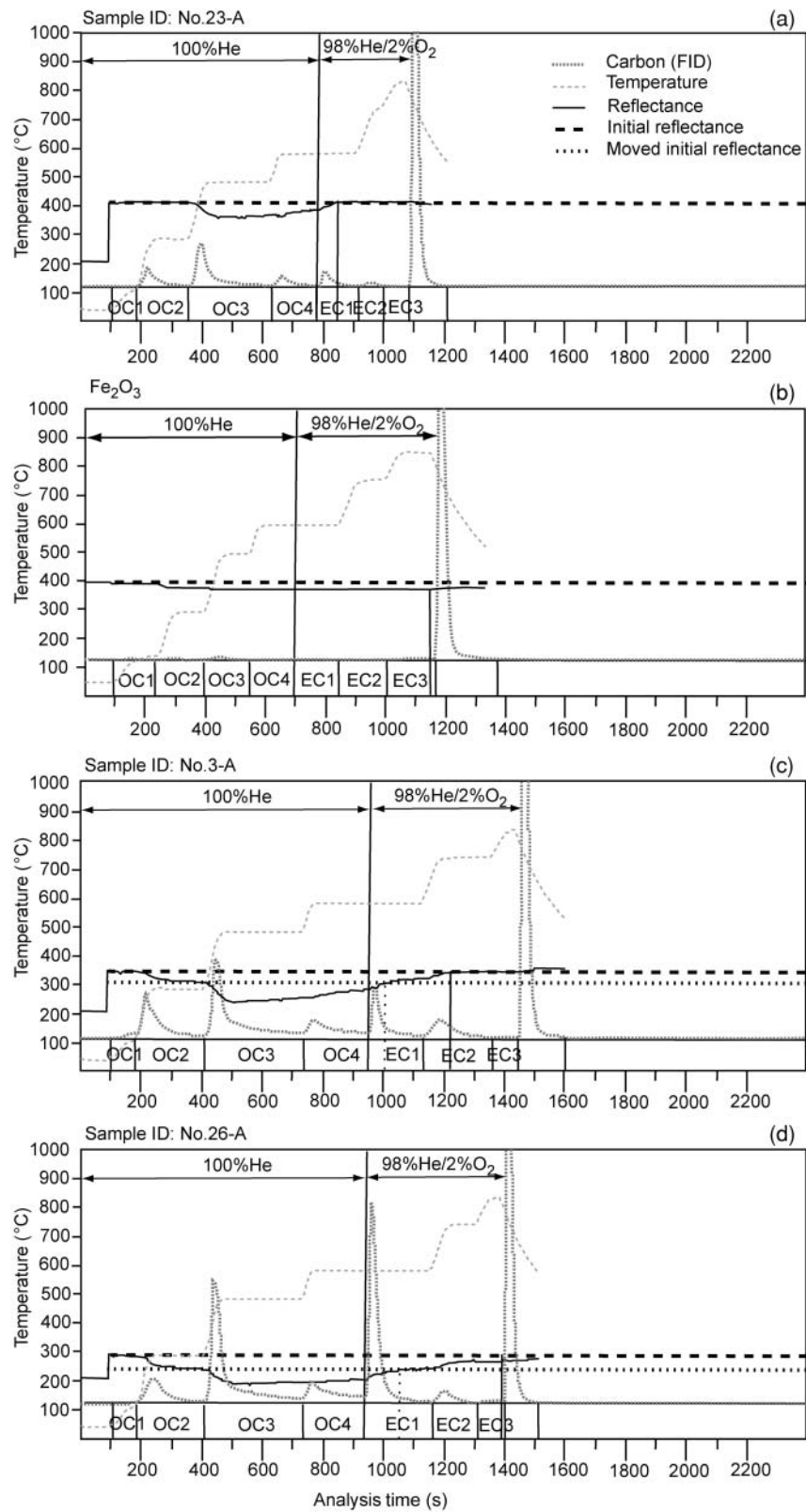


FIG. 2. Example thermograms of No. 23-A (Non-Dust Group), No. 3-A (Dust Group), and No. 26-A (Dust Group) from ice core samples representing 3 kinds of situations with the thermogram of Chemical pure hematite: (a) the laser signal decreases at 450°C and returns back after O₂ is injected; (b) the optical change of Fe₂O₃ when combusted for the second time; (c) the laser signal decreases at 250°C and achieves the original reflectance value at approximately 700°C; and (d) the laser signal decreases at 250°C without returning to the original value.

RESULTS AND DISCUSSION

Ice Samples

Notably, the OC value for No. 8-A and OC and EC values for No. 3-C-II could not be attained because the thermograms were abnormal according to the IMPROVE thermal/optical reflectance (TOR) protocol; as a consequence, these results were considered invalid. The carbon contents on C-I and C-II filters showed that the mean ratio of the OC and EC values on C-II to the corresponding values on both C-I and C-II was 22%, although this ratio is uncertain given the limited number of test cases. Since the carbon value of C-II was relatively smaller compared to the total of C-I and C-II, the OC and EC values of No. 3-C-I were regarded as the total values of the 2 overlapped filters in the following discussion. As a result, twenty-three concentration values for OC were obtained, with 2 undervalued, twenty-four values for EC, with 1 undervalued, and twenty-three values for TC, with 2 undervalued. Values were not blank-corrected, as the purpose of this experiment was to compare the variations among filtering methods.

For the 4 series of datasets, the mean concentrations of OC for F_{ice-A}, F_{ice-B}, F_{ice-C}, and F_{ice-D} were 214.2, 187.8, 143.6, and 170.9 ng g⁻¹, respectively. The mean concentrations of EC were 26.9, 26.4, 26.0, and 18.8 ng g⁻¹, respectively (Table 2). Clearly, F_{ice-A} yielded the highest mean concentrations for OC but did not show statistical difference for EC. In contrast, F_{ice-C} did not exhibit better collection efficiency than the other datasets. There is a good agreement between the mean concentrations of both OC and EC among the 4 sample series sets, with corresponding relative standard deviations (RSDs) of 17% and 16%, respectively.

Figure 3 demonstrates the variations in OC, EC, and TC concentrations along the ice core for all 4 sample series and also depicts the distribution of dust layers. The 4 concentration profiles for OC, EC, and TC are all similar with the exception of the No. 2-B concentrations, which are extremely high compared to the corresponding samples from other filtration methods. These results are indicated by asterisks and will be discussed later. The samples containing visible dust particles are inclined to exhibit relatively high OC and EC values (Figure 3). The OC and EC

TABLE 2
Concentrations (ng g⁻¹) of OC, EC, and TC for ice samples (RSDs (%) are also listed)

Sample No.	OC						EC						TC					
	F _{ice-A}	F _{ice-B}	F _{ice-C}	F _{ice-D}	Mean	RSD ^a	F _{ice-A}	F _{ice-B}	F _{ice-C}	F _{ice-D}	Mean	RSD ^a	F _{ice-A}	F _{ice-B}	F _{ice-C}	F _{ice-D}	Mean	RSD ^a
1	414.3	251.5	<u>217.4</u>	<u>453.6</u>	334.2	35.0	103.2	52.1	<u>35.6</u>	<u>133.2</u>	81.0	55.7	517.5	303.6	<u>253.0</u>	<u>586.8</u>	415.2	39.0
2	346.5	<u>591.6</u>	<u>278.4</u>	293.9	377.6	38.6	40.5	<u>119.3</u>	24.8	<u>18.2</u>	50.7	92.0	387.0	<u>710.9</u>	<u>303.2</u>	312.1	428.3	44.8
3	246.9	267.5	<u>174.0</u>	<u>315.7</u>	251.0	23.4	47.2	<u>71.5</u>	40.7	<u>33.1</u>	48.1	34.5	294.1	339.0	<u>214.7</u>	<u>348.8</u>	299.2	20.4
4	<u>365.6</u>	<u>172.5</u>	197.8	194.8	232.7	38.4	<u>44.5</u>	27.1	37.3	23.2	33.0	29.4	<u>410.1</u>	<u>199.6</u>	235.1	218.0	265.7	36.6
5	133.2	113.5	<u>183.2</u>	<u>111.8</u>	135.4	24.6	11.4	7.7	<u>15.4</u>	6.2	10.2	40.1	144.6	121.2	<u>198.5</u>	<u>118.0</u>	145.6	25.6
6	<u>823.7</u>	710.5	<u>240.1</u>	693.2	616.9	41.8	<u>0.0</u>	<u>0.0</u>	<u>10.3</u>	2.5	3.2	153.2	<u>823.7</u>	710.5	<u>250.5</u>	695.7	620.1	40.8
8		<u>332.9</u>	<u>423.2</u>	392.3	382.8	12.0	<u>75.0</u>	104.8	<u>291.9</u>	75.6	136.8	76.2		<u>437.7</u>	<u>715.1</u>	467.9	540.3	28.2
9	238.2	<u>312.6</u>	<u>159.9</u>	170.0	220.2	32.1	<u>39.9</u>	10.6	<u>10.5</u>	11.9	18.2	79.4	278.1	<u>323.2</u>	<u>170.3</u>	181.9	238.4	31.2
12	<u>280.1</u>	177.1	135.0	<u>122.8</u>	178.8	40.0	<u>39.0</u>	20.1	<u>11.7</u>	15.5	21.6	56.2	<u>319.2</u>	197.2	146.7	<u>138.2</u>	200.3	41.6
13	100.5	<u>153.6</u>	<u>51.9</u>	130.2	109.0	40.2	7.6	<u>62.5</u>	<u>1.6</u>	12.1	21.0	133.7	108.1	<u>216.1</u>	53.5	142.3	130.0	52.4
14	20.6	41.4	26.1	27.1	28.8	30.8	<u>1.1</u>	<u>7.2</u>	4.9	5.6	4.7	54.9	21.7	<u>48.7</u>	31.1	32.8	33.5	33.3
15	27.0	26.9	<u>29.8</u>	<u>22.1</u>	26.4	12.0	<u>7.8</u>	3.0	2.6	4.7	4.5	52.4	<u>34.9</u>	29.9	32.4	26.8	31.0	11.1
16	20.7	<u>27.9</u>	<u>19.4</u>	23.9	23.0	16.5	2.2	4.4	6.3	<u>6.7</u>	4.9	42.1	22.9	<u>32.3</u>	25.7	30.6	27.9	15.6
17	<u>51.2</u>	<u>15.4</u>	32.2	31.0	32.4	45.1	<u>7.3</u>	4.1	5.4	<u>3.6</u>	5.1	32.6	<u>58.4</u>	<u>19.5</u>	37.6	34.5	37.5	42.7
18	<u>152.2</u>	89.8	<u>67.8</u>	81.6	97.8	38.2	<u>13.0</u>	12.1	6.3	7.1	9.6	35.6	<u>165.1</u>	102.0	<u>74.0</u>	88.7	107.5	37.3
19	77.1	<u>55.3</u>	<u>78.1</u>	70.6	70.3	15.0	<u>11.7</u>	8.5	<u>5.0</u>	5.3	7.6	41.3	<u>88.8</u>	<u>63.9</u>	83.1	75.9	77.9	13.8
20	15.7	<u>15.2</u>	<u>24.2</u>	21.9	19.2	23.2	2.8	<u>1.0</u>	<u>3.6</u>	2.2	2.4	44.3	18.6	<u>16.2</u>	<u>27.7</u>	24.1	21.7	24.2
21	<u>36.9</u>	29.2	28.4	20.2	28.7	23.7	<u>8.3</u>	3.5	6.0	<u>1.6</u>	4.9	60.1	<u>45.2</u>	32.8	34.4	21.8	33.5	28.5
22	26.7	27.0	<u>149.6</u>	27.0	57.6	106.6	<u>3.0</u>	4.3	<u>13.3</u>	7.6	7.0	65.4	29.6	31.3	<u>162.8</u>	34.6	64.6	101.5
23	67.7	<u>74.5</u>	55.4	<u>48.7</u>	61.6	19.0	<u>6.5</u>	6.1	3.3	3.7	4.9	33.8	74.2	<u>80.6</u>	58.7	<u>52.4</u>	66.4	19.8
24	<u>277.0</u>	<u>184.9</u>	205.4	238.4	226.4	17.8	<u>52.9</u>	16.5	19.4	<u>15.0</u>	25.9	69.5	<u>329.9</u>	<u>201.4</u>	224.8	253.3	252.4	22.1
25	<u>297.4</u>	174.5	151.4	<u>120.3</u>	185.9	41.7	<u>48.7</u>	14.5	16.0	<u>11.0</u>	22.6	77.7	<u>346.1</u>	189.0	<u>167.5</u>	131.3	208.5	45.5
26	<u>373.5</u>	269.2	<u>236.1</u>	251.9	282.7	21.9	<u>27.2</u>	25.5	24.2	22.7	24.9	7.8	<u>400.7</u>	294.7	<u>260.3</u>	274.6	307.6	20.7
27	<u>533.0</u>	392.9	280.9	238.7	361.4	36.4	<u>44.2</u>	<u>47.6</u>	29.0	22.2	35.8	33.9	<u>577.2</u>	440.5	310.0	<u>260.9</u>	397.2	35.7
Mean	<u>214.2</u>	187.8	<u>143.6</u>	170.9		16.5	<u>26.9</u>	26.4	26.0	<u>18.8</u>		15.7	<u>238.9</u>	214.2	<u>169.6</u>	189.7		14.8
RSD	94.5	96.9	73.6	98.1			99.7	125.5	222.0	153.8			90.2	94.2	89.0	97.4		

^aBetween the 4 series of samples, n = 4. The max and min values for each subsection sample and concentration for Dust Group samples are shown in underline, italic, and shading.

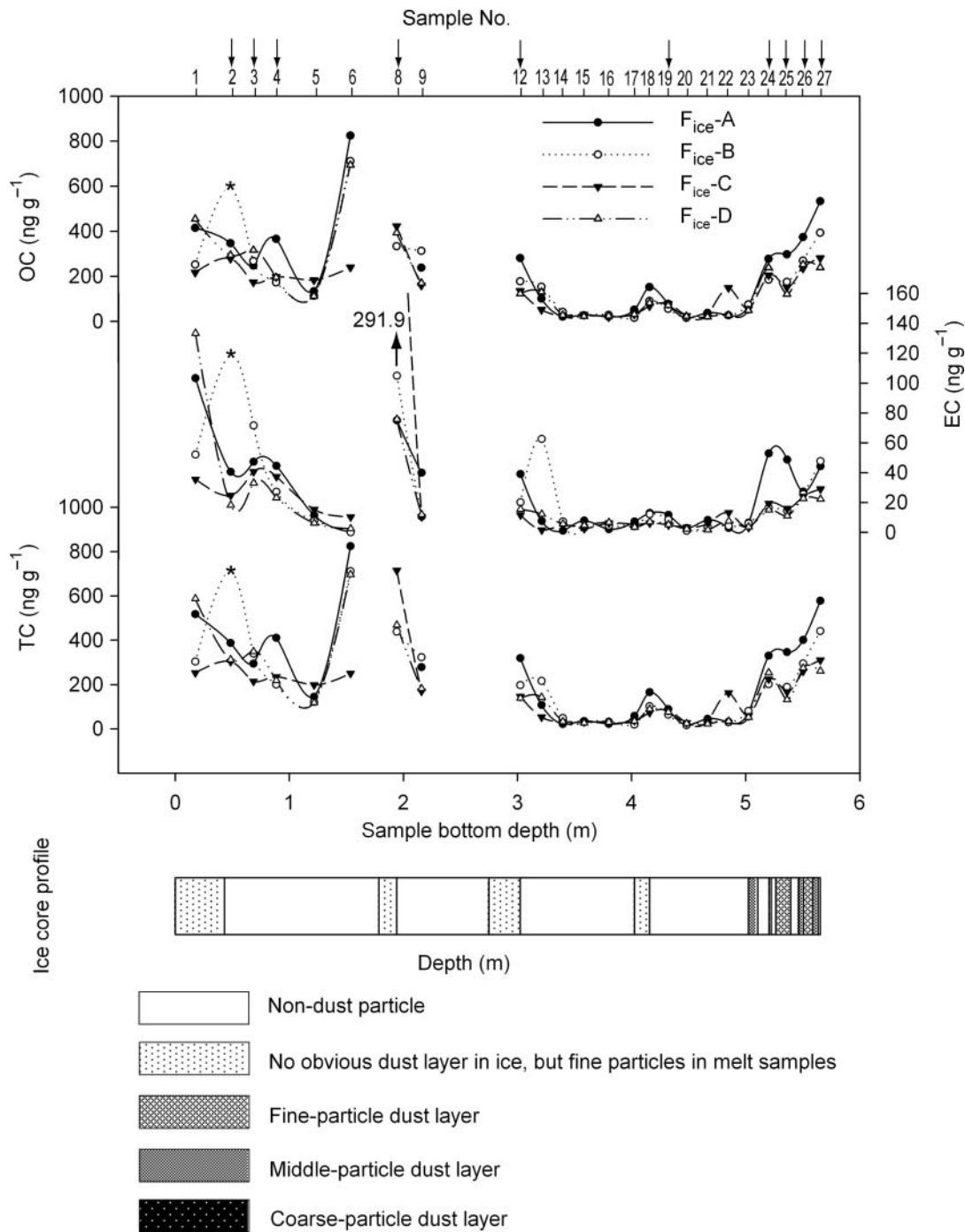


FIG. 3. OC, EC, and TC concentrations for 4 sample series filtered by different methods. The distribution and depiction of dust layers along the ice core are plotted. Outliers sample No. 2-B OC, EC, and TC concentrations shown with asterisks. The sample numbers of the axes labeled with arrows are from the Dust Group; the EC concentration of No. 8-C is 291.9 ng g^{-1} .

averages of 4 filtering methods in the Dust Group are all higher than the corresponding averages in the Non-Dust Group. There are 2 possible explanations for this result based on the assumption that HCl eliminates all carbonates. The first is that the dust, especially the fine particles, and carbonaceous particles in this ice core are transported together during dry seasons (Ming et

al. 2008; Xu et al. 2009a, 2009b). The second possibility is that black carbon and dust in snow concentrate together with sublimation and radiation melting.

The primary aim of this experiment was to determine the difference in magnitude of carbonaceous particle concentrations between the 4 ice core sections with different filtration

TABLE 3
OC, EC, and TC concentrations (ng g^{-1}) for snow sampled at the same elevation and the corresponding RSDs (%)

Elevation of snow sample (m)	OC					EC					TC				
	$F_{\text{snow-A}}$	$F_{\text{snow-B}}$	$F_{\text{snow-C}}$	Mean	RSD	$F_{\text{snow-A}}$	$F_{\text{snow-B}}$	$F_{\text{snow-C}}$	Mean	RSD	$F_{\text{snow-A}}$	$F_{\text{snow-B}}$	$F_{\text{snow-C}}$	Mean	RSD
5300	<u>185.9</u>	<u>186.9</u>	<u>196.5</u>	189.8	3.1	5.5	<u>5.8</u>	2.9	4.7	34.1	<u>191.4</u>	<u>192.7</u>	<u>199.4</u>	194.5	2.2
5200	<u>139.9</u>	<u>176.4</u>	<u>154</u>	156.8	11.7	2.7	<u>3</u>	1.1	2.3	45.7	<u>142.7</u>	<u>179.4</u>	<u>155.1</u>	159	11.8
5100	<u>85.6</u>	<u>121.6</u>	<u>91.6</u>	99.6	19.4	6	<u>7.5</u>	4.3	5.9	27.3	<u>91.6</u>	<u>129.1</u>	<u>95.8</u>	105.5	19.5
5000	<u>73.7</u>	<u>98</u>	<u>94.9</u>	88.9	14.9	1.5	<u>4.1</u>	1.5	2.3	64.4	<u>75.2</u>	<u>102.1</u>	<u>96.4</u>	91.2	15.6
4900	<u>163.4</u>	<u>220.3</u>	<u>90</u>	158.1	41.5	6.6	<u>11.4</u>	5.1	7.7	42.8	<u>169.9</u>	<u>232.3</u>	<u>95.1</u>	165.8	41.4
4800	<u>453.6</u>	<u>531.3</u>	<u>292.8</u>	425.9	28.6	79.6	<u>100.4</u>	<u>51.6</u>	77.2	31.7	<u>533.2</u>	<u>631.6</u>	<u>344.4</u>	503.1	29
Mean	<u>183.7</u>	<u>222.5</u>	<u>153.3</u>		18.6	17.0	<u>22.0</u>	<u>11.1</u>		32.9	<u>200.7</u>	<u>244.5</u>	<u>164.4</u>		19.8

The max and min values for each elevation snow sample are shown in underline and italic.

methods. These particles are derived from the original aerosol deposition, which was primarily determined by analyzing the variability of OC and EC concentration values between the ice core subsections in the Non-Dust Group. As mentioned above, $F_{\text{ice-A}}$, $F_{\text{ice-B}}$, and $F_{\text{ice-D}}$ could be regarded as repeats because the sections from the Non-Dust Group did not contain visible dust particles in the meltwater. The discrepancies between the 3 series of samples for both the OC and EC were not statistically significant when tested by one-way analysis of variance (ANOVA), and the RSDs of the average OC and EC concentrations were both $\leq 10\%$. Furthermore, statistically significant correlations were observed among 3 concentration data series at the 0.01 significance level (two-tailed) for OC and at the 0.05 significance level for EC. The correlations were stronger if the EC value for sample No. 13-B was eliminated. Thus, the small discrepancies between OC and EC concentrations from the $F_{\text{ice-A}}$, $F_{\text{ice-B}}$, and $F_{\text{ice-D}}$ filtering methods were not due to a systematic measurement error, but instead could be attributed to the heterogeneity in the distribution of carbonaceous particles within the ice core cross-sections. In addition, the variability in carbonaceous particles between the core slabs was substantially higher with the presence of dust layers.

Correlation analysis was also applied in the Dust Group between $F_{\text{ice-A}}$ and $F_{\text{ice-B}}$ and between $F_{\text{ice-B}}$ and $F_{\text{ice-D}}$. No statistically significant correlation was present at the 0.01 significance level, however, with the values of sample No. 2-B eliminated, the correlation coefficients for both OC and EC were significant ($\alpha = 0.05$) for both $F_{\text{ice-A}}$ and $F_{\text{ice-B}}$ and for $F_{\text{ice-B}}$ and $F_{\text{ice-D}}$. The OC and EC values of No. 2-B were outliers and were excluded from the following discussion and analysis.

The high correlation between $F_{\text{ice-A}}$ and $F_{\text{ice-B}}$ in the Dust Group indicates that carbonaceous particle concentrations present similar variation trends independent of whether the dust is collected on the filters or not. Despite the initial discrepancies in carbonaceous particle content between the 4 sample series in this group, $F_{\text{ice-A}}$ was prone to obtain the highest OC and EC concentrations among the 4 series (Table 2; Figure 3). Variance analysis demonstrated no significant difference ($\alpha = 0.05$) between $F_{\text{ice-B}}$, $F_{\text{ice-C}}$, and $F_{\text{ice-D}}$, nor among all 4 fil-

tering methods. These results showed that some carbonaceous particles might attach to dust particles, although it did not result in a statistically significant difference after the data adjustment outlined in previous section.

For both the OC and EC concentrations, the values for the $F_{\text{ice-D}}$ samples did not deviate significantly from $F_{\text{ice-B}}$ (Figure 3) and the correlation coefficients between $F_{\text{ice-B}}$ and $F_{\text{ice-D}}$ were significant at the 0.05 level. The EC data from the $F_{\text{ice-D}}$ samples exhibited no significant difference from $F_{\text{ice-B}}$, but did differ significantly from the $F_{\text{ice-A}}$ samples ($P = 0.03$). There was no significant difference between $F_{\text{ice-B}}$ and $F_{\text{ice-A}}$ as determined via ANOVA. These results indicated that some carbonaceous particles did attach to dust particles, and mechanical stirring with a glass bar was insufficient in fully detaching the carbonaceous matter.

Snow Samples

Sonication was used on a series of snow samples to better achieve separation of carbonaceous particles from dust and to quantify the amount of carbonaceous particles attached to dust. Among all 3 series of datasets from different filtration methods,

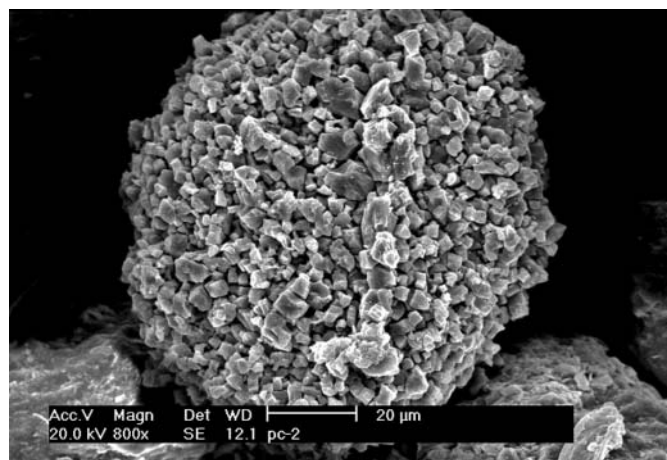


FIG. 4. An SEM image illustrating the aggregates of dust in a Noijin Kangsang surface snow sample after filtration.

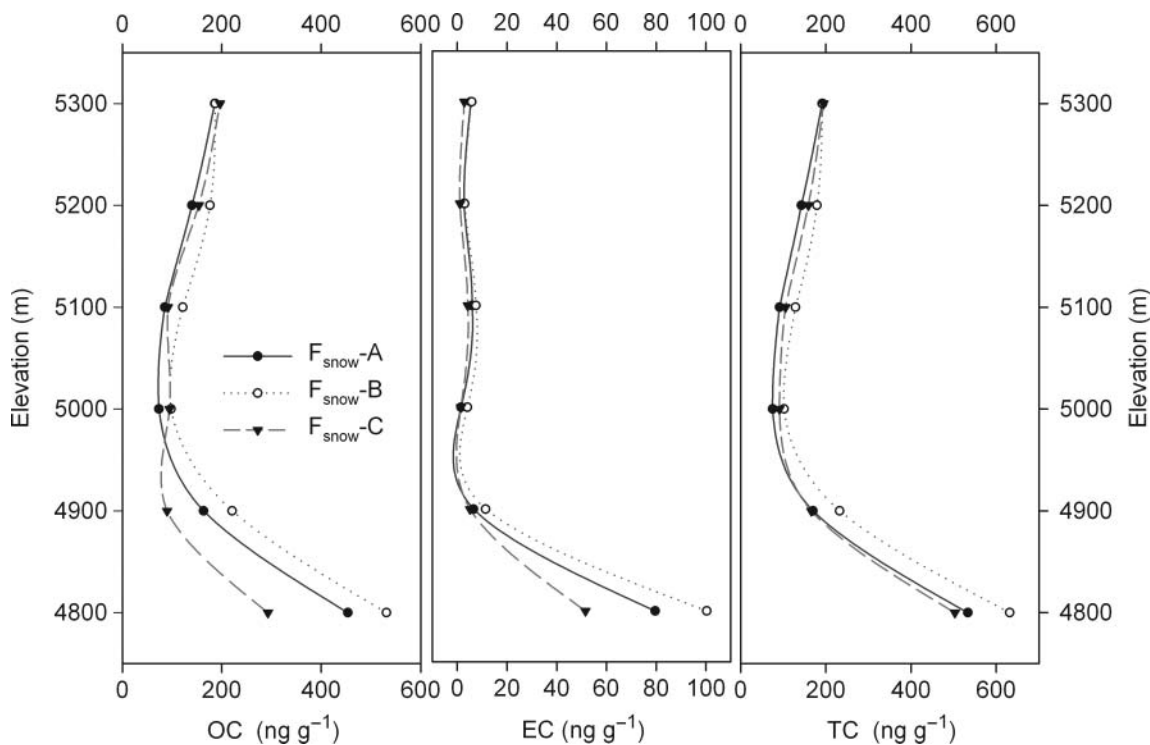


FIG. 5. OC, EC, and TC concentrations of snow sampled at different elevations using different filtering methods.

$F_{\text{snow-B}}$ always yielded the highest concentrations, except for the OC value of the sample from 5300 m a.s.l. (Table 3). Notably, the EC concentrations exhibited the order $F_{\text{snow-B}} > F_{\text{snow-A}} > F_{\text{snow-C}}$. The same regularities were also found for the mean concentrations of both OC and TC. The relative standard deviation between methods was 19% for OC, 33% for EC, and 20% for TC. No significant difference was found among the 3 series of datasets using ANOVA.

Although insoluble particles were filtered in the $F_{\text{snow-A}}$ samples, the maximum value for TC was not obtained. These results indicated that only a part of the carbonaceous particles were released and subsequently analyzed with the Thermal/Optical Carbon Analyzer. The incomplete combustion may be related to the morphology of particles on the filter and the analysis procedures.

As meltwater flows away or evaporates in snow-firn pack, the carbonaceous matter and dust particles can accumulate with black carbon incorporated into larger agglomerates, comprised mostly of dust (Figure 4). When the particles were combusted in the analyzer after filtration, the black carbon attached on the cluster surface could be successfully oxidized at every temperature/atmosphere condition. However, the oxidization and release of carbonaceous particles inside would be at a low speed because of the aggregate structure. On the other hand, when the FID response returns to baseline or remains at a constant value for a certain time in the thermal/optical carbon analysis system, temperature/atmosphere begins in the next analysis stage (Chow

et al. 1993, 2004). Therefore, when carbon volatilized slowly from the filter at a constant speed, the next analysis stage began although the carbon had not yet been completely oxidized. In contrast to $F_{\text{snow-A}}$, $F_{\text{snow-B}}$ might have broken the black carbon and dust clusters into smaller pieces and detached the fine carbonaceous particles from dust into the meltwater via ultrasonic agitation. The suspended particles in the meltwater were then more effectively combusted at relatively high speed after collection on the filters. Furthermore, the filter sample of $F_{\text{snow-B}}$ spent a longer time than $F_{\text{snow-A}}$ in the analysis as FID could detect efficient carbon content to keep each analysis stage proceeding. Therefore, we suggest $F_{\text{snow-B}}$ was able to produce more carbon than $F_{\text{snow-A}}$ and exhibit relatively “complete” carbon concentrations.

In order to illustrate that the aggregation can be destroyed by ultrasonic agitation, the particle sizes in 2 melt snow samples (from 4800 and 4900 m a.s.l) were analyzed by Multisizer™ 3 COULTER COUNTER before and after sonication. The results showed that the mean particle diameter decreased by about 17% with ultrasonic agitation. Relatively smaller particles more efficiently detached black carbon from dust.

By comparing $F_{\text{snow-B}}$ and $F_{\text{snow-C}}$, the amount of carbonaceous particles attached to dust could be ascertained, given the assumption that ultrasonic agitation detaches all of the black carbon from the dust particles. The mean OC, EC, and TC values of the snow samples from $F_{\text{snow-B}}$ were 31%, 50%, and 33% higher than those from $F_{\text{snow-C}}$, respectively.

The impact of dust–BC agglomerates from snow aging on carbonaceous particle concentration analysis was augmented in the surface snow samples with decreasing elevation due to enhanced melting. As a consequence, the differences in OC and EC concentrations between the 3 methods increased (Table 3, Figure 5).

CONCLUSIONS

One ice core was cut into 4 columns with each column corresponding to a different method ($F_{\text{ice-A}}$, $F_{\text{ice-B}}$, $F_{\text{ice-C}}$, and $F_{\text{ice-D}}$) for filtering carbonaceous particles. Six surface snow samples with differing dust concentrations, which were sampled along an elevation gradient on a glacier, were analyzed using 3 different methods ($F_{\text{snow-A}}$, $F_{\text{snow-B}}$, and $F_{\text{snow-C}}$), including samples filtered after sonication.

It can be assumed that the effect on the reflectance signal from dust can be eliminated by altering the original reflectance value line to the reflectance value directly after the 250°C stage in the thermal/optical method of carbon analysis. The differences among the 4 methods indicate that black carbon attaches to dust particles and mechanical stirring alone is insufficient in separating the aggregates. Furthermore, the ineffectiveness of a single filter for collecting carbonaceous particles is demonstrated from the loss of very small carbonaceous particles during filtration.

The method of sonicating snow samples results in the maximum values of black carbon among the 3 different datasets, although settling is eliminated from the analysis. We hypothesize that ultrasonic agitation is effective in destroying dust–BC aggregate structures created from snow aging, thus promoting carbon volatilization with the thermal/optical method.

To the extent suggested by these results, it is recommended that the filtration process of ice and snow samples for the measurement of carbonaceous particle concentrations include the following: Oscillate melted samples by ultrasonic agitation for 15 min to destroy the dust–BC aggregates and allow samples to settle for about 15 min before pipetting the supernatant for filtering through a single quartz filter.

REFERENCES

- Birch, M. E. (1998). Analysis of Carbonaceous Aerosols: Interlaboratory Comparison. *The Analyst*, 123:851–857.
- Cachier, H., and Pertuisot, M. (1994). Particulate Carbon in Arctic Ice. *Analysis*, 22(7):34–37.
- Cao, J. J., Lee, S. C., Ho, K. F., Zhang, X. Y., Zou, S. C., Fung, K., Chow, J. C., and Watson, J. G. (2003). Characteristics of Carbonaceous Aerosol in Pearl River Delta Region, China During 2001 Winter Period. *Atmos. Environ.*, 37:1451–1460.
- Cao, J. J., Zhu, C. S., Chow, J. C., Liu, W. G., Han, Y. M., and Watson, J. G. (2008). Stable Carbon and Oxygen Isotopic Composition of Carbonate in Fugitive Dust in the Chinese Loess Plateau. *Atmos. Environ.*, 42:9118–9122.
- Chow, J. C., and Watson, J. G. (2002). PM_{2.5} Carbonate Concentrations at Regionally Representative Interagency Monitoring of Protected Visual Environment Sites. *J. Geophys. Res.*, 107:8344.
- Chow, J. C., Watson, J. G., Chen, L. W. A., Arnott, W. P., Moosmiller, H., and Fung, K. (2004). Equivalence of Elemental Carbon by Thermal/Optical Reflectance and Transmittance with Different Temperature Protocols. *Environ. Sci. Technol.*, 38:4414–4422.
- Chow, J. C., Watson, J. G., Crow, D., Lowenthal, D. H., and Merrifield, T. (2001). Comparison of IMPROVE and NIOSH Carbon Measurements. *Aerosol Sci. Technol.*, 34:23–34.
- Chow, J. C., Watson, J. G., Pritchett, L. C., Pierson, W. R., Frazier, C. A., and Purcell, R. G. (1993). The DRI Thermal/Optical Reflectance Carbon Analysis System: Description, Evaluation and Applications in U. S. Air Quality Studies. *Atmos. Environ.*, 27A:1185–1201.
- Clarke, A. D., and Noone, K. J. (1985). Soot in the Arctic Snowpack: A Cause for Perturbations in Radiative Transfer. *Atmos. Environ.*, 19:2045–2053.
- Cong, Z. Y., Kang, S. C., Dong, S. P., Liu, X. D., and Qin, D. H. (2008). Elemental and Individual Particle Analysis of Atmospheric Aerosols from High Himalayas. *Environ. Monit. Assess.*, 160:323–335.
- Countess, R. (1990). Interlaboratory Analyses of Carbonaceous Aerosol Samples. *Aerosol Sci. Technol.*, 12:114–121.
- Hansen, A. D. A., Kapustin, V. N., Kopeikin, V. M., Gillette, D. A., and Bodhaine, B. A. (1993). Optical Absorption by Aerosol Black Carbon and Dust in a Desert Region of Central Asia. *Atmos. Environ.*, 27A:2527–2531.
- Hansen, A. D. A., Rosen, H., and Novakov, T. (1984). The Aethalometer: An Instrument for the Real-Time Measurement of Optical Absorption by Aerosol Particles. *Sci. Total. Environ.*, 36:191–196.
- Hansen, J., and Nazarenko, L. (2004). Soot Climate Forcing via Snow and Ice Albedos. *Proc. Natl. Acad. Sci. USA*, 101(2):423–428.
- Lavanchy, V. M. H., Gäggeler, H. W., Schotterer, U., Schwikowski, M., and Baltensperger, U. (1999). Historical Record of Carbonaceous Particle Concentrations from a European High-Alpine Glacier (Colle Gnifetti, Switzerland). *J. Geophys. Res.*, 104:21227–21236.
- Lioussé, C., Cachier, H., and Jennings, S. G. (1993). Optical and Thermal Measurements of Black Carbon Aerosol Content in Different Environments: Variation of the Specific Attenuation Cross-Section, Sigma (σ). *Atmos. Environ.*, 27A:1203–1211.
- McConnell, J. R., Edwards, R., Kok, G. L., Flanner, M. G., Zender, C. S., Saltzman, E. S., Banta, J. R., Pasteris, D. R., Carter, M. M., and Kahl, J. D. W. (2007). 20th-Century Industrial Black Carbon Emissions Altered Arctic Climate Forcing. *Science*, 317:1381–1384.
- Ming, J., Cachier, H., Xiao, C., Qin, D., Kang, S., Hou, S., and Xu, J. (2008). Black Carbon Record Based on a Shallow Himalayan Ice Core and Its Climatic Implications. *Atmos. Chem. Phys.*, 8(5):1343–1352.
- Puxbaum, H., and Bauer, H. (2001) International Aerosol Round Robin Test Stage I and II, and Other Studies of Organic Aerosol Chemistry at the CTA. http://aerosol.web.psi.ch/Final_reports/18%20%20Puxbaum.pdf
- Ramanathan, V., and Carmichael, G. (2008). Global and Regional Climate Changes Due to Black Carbon. *Nat. Geosci.*, 1(4):221–227.
- Schmid, H., Laskus, L., Abraham, H. J., Baltensperger, U., Lavanchy, V., Bizjak, M., Burba, P., Cachier, H., Crow, D., Chow, J., Gnauk, T., Even, A., ten Brink, H. M., Giesen, K.-P., Hitznerberger, R., Hueglin, C., Maenhaut, W., Pio, C., Carvalho, A., Putaud, J.-P., Toom-Saunt, D., and Puxbaum, H. (2001). Results of the Carbon Conference International Aerosol Carbon Round Robin Test Stage I. *Atmos. Environ.*, 35:2111–2121.
- Warren, S. G., and Clarke, A. D. (1990). Soot in the Atmospheric and Snow Surface of Antarctica. *J. Geophys. Res.*, 95:1811–1816.
- Xu, B., Cao, J., Hansen, J., Yao, T., Joswila, D. R., Wang, N., Wu, G., Wang, M., Zhao, H., Yang, W., Liu, X., and He, J. (2009a). Black Soot and the Survival of Tibetan Glaciers. *Proc. Natl. Acad. Sci. USA*, 106(52):22114–22118.
- Xu, B., Wang, M., Joswiak, D. R., Cao, J., Yao, T., Wu, G., Yang, W., and Zhao, H. (2009b). Deposition of Anthropogenic Aerosols in a Southeastern Tibetan Glacier. *J. Geophys. Res.*, 114:D17209.
- Xu, B. Q., Yao, T. D., Liu, X. Q., and Wang, N. L. (2006). Elemental and Organic Carbon Measurements with a Two-Step Heating Gas Chromatography System in Snow Samples from the Tibetan Plateau. *Ann. Glaciol.*, 43:257–262.